ACES Asian Chemical Editorial Society
DOI: 10.1002/asia.202100125
CHEMISTRY
AN ASIAN JOURNAL
Communication

Surface Functionalization of a γ-Graphyne-like Carbon Material via Click Chemistry

Huatian Xiong+,[a] Haiyuan Zou+,[b] Hong Liu,[a] Mei Wang,[a] and Lele Duan*[a, b]

Abstract: Surface functionalization of carbon materials is of interest in many research fields, such as electrocatalysis, interfacial engineering, and supercapacitors. As an emerging carbon material, γ-graphyne has attracted broad attention. Herein, we report that the surface functionalization of a γ-graphyne-like carbon material (**γ-G1**) is achieved by immobilizing functional groups via the click chemistry. Texture analysis of aberration-corrected microscopy, X-ray photoelectron spectroscopy, and electrochemistry confirm the successful surface modification of **γ-G1** through a strong covalent linkage 1,2,3-triazole. The direct linkage of functional groups on **γ-G1** via the click chemistry represents a general method for preparing other functional materials by using γ-graphyne-like materials as a skeleton.

Surface functionalization is one of the powerful methods to prepare host materials with desired merits and is currently adapted in various processes.[1–5] Especially, the immobilization of homogenous molecules/complexes on heterogeneous substrates is expected to combine the advantages of both homogenous and heterogeneous systems, providing advanced hybrid materials.[6–8] The surface-immobilized molecules/complexes usually feature well-defined structures at the atomic level, and their structures and functions are readily tunable, imposing competent characteristics on host materials.

From the viewpoint of molecular interaction forces, surface immobilization strategies can be briefly summarized as follows: (i) covalent attachment, (ii) electrostatic interactions, (iii) hydrogen bonding, (iv) van der Waals forces involved in the physisorption of molecules on solid surfaces, and (v) physical entrapment inside pores.[9–14] Prevalently, most decorated molecules stabilized on the substrate surface undergo weak interactions like electrostatic adsorption or van der Waals attraction. For example, on the typical carbonaceous material of graphite, graphene, and carbon nanotubes, the immobilization of molecular modifiers is primarily achieved by π-π interaction or hydrophobic forces, which can dramatically change the physicochemical characteristics of the host materials, making them promising candidates in various fields.[15–17] In comparison, the covalent bond can certainly provide a stronger interlinkage between modifiers and host materials, reinforcing the stability of the bounded molecules and further broadening their applications, particularly under harsh operating conditions.[18] Nevertheless, surface functionalization of the aforementioned carbonaceous materials via the covalent interaction is synthetically challenging due to the inert nature of benzene rings and lack of reactive ligands on the surface; introducing additional specific functional groups, such as $-NH_2$, $-CN$ and $-COOH$, is then required, as shown in Scheme 1a and 1b.[19–21] Therefore, seeking a new carbon material with intrinsic reactive groups to establish a strong covalent interaction with surface modifiers is desired but remains largely elusive.

Graphyne, as a newly emerging two-dimensional carbon allotrope and constituted of sp^2-hybridized benzene rings and sp-hybridized alkyne linkages, has gained increasing attention due to their fascinating structures and properties.[22–31] According to the difference in construction, the graphyne family can be classified into a series of subtypes, including α-, β-, γ-graphyne, graphdiyne, and 6,6,12-graphyne.[32–35] Within these frameworks, the acetylenic linkages enable the possible chemical reaction with introduced molecules through mature reactions, such as the Diels-Alder reactions and the click reactions.[36,37] Up to now, the proof-of-concept study on covalent attachment of homogeneous molecules/complexes on graphyne has yet to be tapped, and we report herein the synthesis of defective γ-graphyne-like carbonaceous (**γ-G1**) with

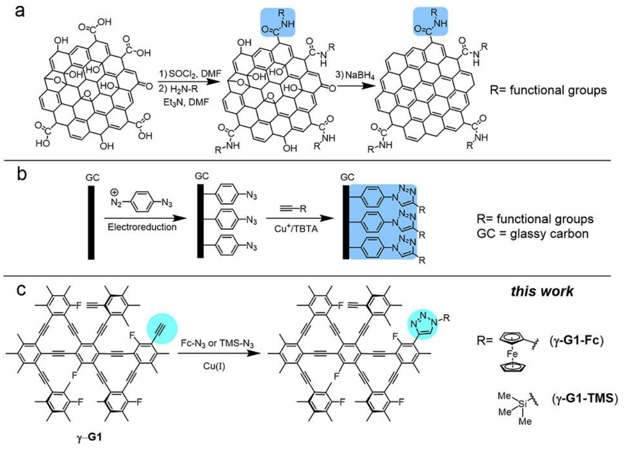

Scheme 1. Some examples of surface modification by covalent bonding. (a) Reprinted from Ref. 20; (b) reprinted from Ref. 21; (c) this work.

---

[a] H. Xiong,+ H. Liu, Prof. Dr. M. Wang, Prof. Dr. L. Duan
State Key Laboratory of Fine Chemicals
Dalian University of Technology
Dalian, 116024, P. R. China

[b] H. Zou,+ Prof. Dr. L. Duan
Department of Chemistry and Shenzhen Grubbs Institute
Southern University of Science and Technology
Shenzhen, 518055, P. R. China
E-mail: duanll@sustech.edu.cn

[+] These authors contributed equally.

Supporting information for this article is available on the WWW under https://doi.org/10.1002/asia.202100125 terminal alkyne groups and the first successful covalent surface functionalization via click reactions.

The α-carbon in fluorobenzene can react with nucleophilic reagents, due to the strong electronegativity of F.[38] Therefore, the γ-graphyne-like carbonaceous **γ-G1** was prepared through the solvothermal treatment of the deprotonated 1,3,5-triethynyl-2,4,6-trifulorobenzene (Scheme S1, Figures S1–S6) via the aromatic nucleophilic substitution of Ar–F by the Ar–C≡C$^-$ anion (Scheme 2). The XPS analysis of the resulting **γ-G1** (Table S1) showed a very low F:C ratio of 1:83, in line with the leaving of F from the aromatic ring; in addition, the F$^-$ anion generated from the reaction was detected by the ion chromatography (Figure S7), confirming the nucleophilic substitution pathway. The as-prepared **γ-G1** material was characterized by Raman and XPS (see details below) and these results are in agreement with the proposed γ-graphyne-like structure.[32] The presence of terminal, unreacted alkyne groups in the as-prepared **γ-G1** allowed us to carry out the surface modification reaction with azide compounds via the well-known click chemistry. As a proof-of-concept study, two azide compounds, azidoferrocene (Scheme S2) and trimethylsilyl azide, were immobilized on **γ-G1** through the 1,2,3-triazole linkage formed via the click reaction, yielding two functionalized materials **γ-G1-Fc** and **γ-G1-TMS** (Scheme 1c), respectively.

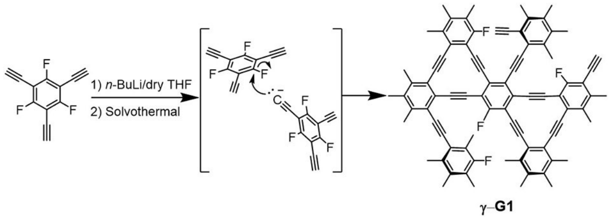

Scheme 2. The synthetic scheme of **γ-G1**.

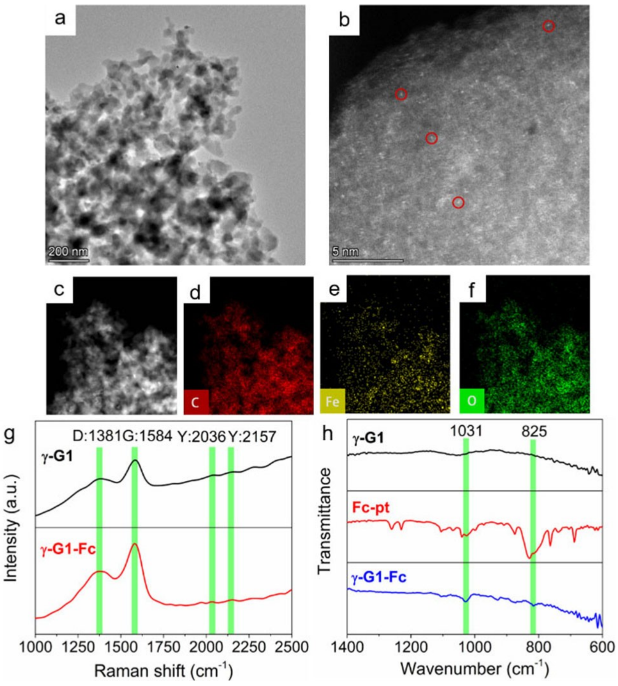

Figure 1. (a) TEM image of **γ-G1**; (b) HAADF-STEM and (c-f) EDS images of **γ-G1-Fc**; (g) Raman spectrum of **γ-G1** and **γ-G1-Fc**; (h) FT-IR spectrum of **γ-G1**, **Fc-pt**, and **γ-G1-Fc**.

The morphology of **γ-G1** was investigated by transmission electron microscopy (TEM; Figure 1a), revealing a porous structure. The energy dispersive spectrometry (EDS) images of **γ-G1** show certain amounts of element F (Figure S8), suggesting that the aromatic nucleophilic substitution reaction is not complete and **γ-G1** should contain abundant terminal alkyne groups. In addition, the nitrogen adsorption-desorption studies were carried out to evaluate the porosity of **γ-G1** (Figure S9). The material of **γ-G1** exhibits the type IV isotherm with the pore size distribution in the range of 0.6 nm, 1.3 nm, and 34.0 nm, indicating the microporous and mesoporous structure of **γ-G1**. The Brunauer-Emmett-Teller (BET) surface area is 788.05 $m^2 g^{-1}$. Besides, high-angle annular dark-field scanning transmission electron microscopy (HAADF-STEM) of **γ-G1-Fc** clearly shows that the element Fe was distributed uniformly in **γ-G1-Fc** (Figure 1b), which is consistent with the EDS images (Figure 1c–f).

Raman spectra of **γ-G1** and **γ-G1-Fc** smoothed by FFT filter are presented in Figure 1g (unsmoothed spectra shown in Figure S10). The D band at around 1381 cm^{-1} corresponds to the structure defects, including the amorphous carbon atoms and edges.[36] The strong G band at around 1584 cm^{-1} represents the stretching vibration of sp^2 hybridized carbon atoms in benzene rings, suggesting that the samples possess abundant benzene rings. Two weak bands at around 2036 cm^{-1} and 2157 cm^{-1} are ascribed to the stretching vibration of *sp* hybridized carbon atoms in the acetylene group. The Raman spectrum of the as-prepared **γ-G1** is consistent with that of γ-graphyne reported by the Cui group, revealing the γ-graphyne-like nature of **γ-G1**.[32,35,39] No obvious difference was noticed between Raman spectra of **γ-G1** and **γ-G1-Fc**, suggesting that their main structures of these two materials are the same. Fourier transform infrared spectroscopy (FT-IR) demonstrated strong evidence for the successful immobilization of Fc groups. As shown in Figure 1h, the bands at 825 cm^{-1} and 1031 cm^{-1} are due to the vibration of C–H bonds of the Cp rings of ferrocene. These two vibrational bands were observed for **γ-G1-Fc** but not for **γ-G1**.

Besides, X-ray photoelectron spectroscopy (XPS) technology was performed to provide more information about the elementary composition and bonding structure of **γ-G1** and **γ-G1-Fc**. The atomic ratio of elements C and F in the XPS spectrum of **γ-G1** (83:1) is much larger than that of 1,3,5-triethynyl-2,4,6-trifulorobenzene in theory (4:1). The XPS surveys in Figure 2a showed that the **γ-G1** and **γ-G1-Fc** are mainly composed of carbon and oxygen, while a small amount of nitrogen and iron elements (2.67% and 0.94% atoms, respectively) were detected in **γ-G1-Fc**. The XRD data also confirm that **γ-G1** is a carbon material (Figure S11). The C 1s XPS spectrum of **γ-G1** in Figure 2b could be fitted into four subpeaks located at 284.5, 285.2, 286.6, and 288.5 eV, which can be assigned to the C 1s orbitals of C–C(sp^2), C–C(*sp*), C–F and C=O, respectively. The presence of element O in C=O drives from the adsorbed oxygen on the surface or the oxidized group

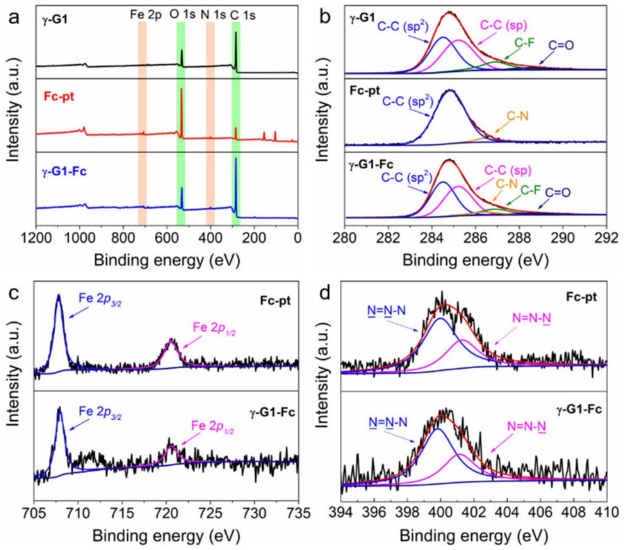

Figure 2. (a) XPS surveys spectra and (b) C 1s XPS spectra of **γ-G1**, **Fc-pt**, and **γ-G1-Fc**; (c) Fe 2*p* and (d) N 1s XPS spectra of **Fc-pt**, and **γ-G1-Fc**.

of some exposed terminal alkyne groups, as previously reported in carbon materials.[40,41] Notably, the area ratio of the sp^2 and *sp* hybridized carbon atoms in **γ-G1** is 0.99, suggesting that **γ-G1** has almost the same carbon composition with γ-graphyne. For **γ-G1-Fc**, the subpeaks deconvoluted from **γ-G1** together with a subpeak at 286.4 eV due to the C–N were considered in the fitting. To our delight, the area ratio of the sp^2 and *sp* hybridized carbon atoms in **γ-G1-Fc** is slightly higher than that in **γ-G1** (1.01 versus 0.99). This is due to that (i) the sp^2 hybridized carbon atoms of the Cp rings in the ferrocene are introduced and (ii) some *sp* hybridized carbon atoms in terminal alkyne groups were transformed into the sp^2 hybridized carbon atoms in triazole.

The oxidation state of Fe in **γ-G1-Fc** was determined by comparing the Fe 2*p* XPS spectra between **Fc-pt** and **γ-G1-Fc** (Figure 2c). The two spin-orbit components Fe 2$p_{3/2}$ and Fe 2$p_{1/2}$ of **Fc-pt** and **γ-G1-Fc** are almost the same, all at around 707.8 eV and 720.5 eV, respectively. Thereby, the oxidation state of Fe in **γ-G1-Fc** is $+2$.[42,43]

Most importantly, the N 1s XPS spectra of **γ-G1-Fc** and **Fc-pt** further prove the hypothesis that the attachment of the azidoferrocene on **γ-G1** is via the click reaction (Figure 2d). Two subpeaks (399.96 eV and 401.26 eV) of **γ-G1-Fc** can be deconvoluted from the N 1s XPS spectrum. Those two subpeaks are associated with the photoelectron emission from nitrogen atoms of the immobilized triazole moiety,[44,45] and can be ascribed to the sp^2 and sp^3 N atoms, which are almost identical to the subpeaks of the N 1s spectrum of **Fc-pt** (399.82 eV and 401.12 eV). The ratio of the subpeaks area is close to 2, which is consistent with the structure of triazole in theory. If the azidoferrocene was physically adsorbed on the **γ-G1**, the N 1s signal should be found at ~403 eV, which could not be detected or fitted in the N 1s peak of **γ-G1-Fc**.[44]

To further confirm that the attachment of the azidoferrocene via click reaction is successful, the electrochemistry of **γ-G1-Fc** was studied. Figure 3 shows the cyclic voltammetry (CV) of **γ-G1-Fc** and **γ-G1** in 1.0 M HClO$_4$. The CV of **γ-G1-Fc** shows well-behaved oxidation and reduction waves at 0.596 V and 0.460 V vs. Ag | AgCl | 3 M KCl. These redox peaks are closed to the redox peaks of **Fc-pt** (0.555 V and 0.508 V vs. Ag | AgCl | 3 M KCl) under the same conditions (Figure S12), confirming the formation of triazole and the electrochemical activity of **γ-G1-Fc**.

Another azide, trimethylsilyl azide that is commercially available was used to test the generality of the click reaction on **γ-G1**, and the XPS was performed to study the corresponding product (**γ-G1-TMS**). Due to the low load of trimethylsilyl azide (about 0.37% of Si atoms), the Si 2*p* signal in the XPS survey of **γ-G1-TMS** is weak but a more obvious N 1s signal can be detected (Figure S13a). The C 1s XPS spectrum can be deconvoluted into six subpeaks including C–N (286.4 eV), C–Si (285 eV), and the subpeaks from **γ-G1** (Figure S13b). Besides, the weak peak in the Si 2*p* XPS spectrum was attributed to Si–C (102.3 eV) (Figure S13c).[46] The formation of triazole was confirmed by the N 1s XPS spectrum that was fitted into two subpeaks (399.71 eV and 401.01 eV), and the area ratio of those two subpeaks is around 2 (Figure S13d). Apparently, the click reaction has a broad substrate scope on **γ-G1**. Immobilization of transition metal complexes-based molecular catalysts (such as carbon dioxide reduction catalysts and water splitting catalysts) on **γ-G1** (Figure 4) is ongoing.

In conclusion, a γ-graphyne-like carbon material, **γ-G1**, was synthesized by the aromatic nucleophilic substitution reaction and surface functionalization of **γ-G1** via click reaction was successfully demonstrated. Various techniques, such as HAADF-STEM, XPS, IR, Raman, and CV, were employed to confirm the attachment of functional groups and the formation of the triazole-based covalent linkage. This study has paved the way to functionalize graphyne-based carbon materials using azide compounds via the click reaction, and the resulting hybrid materials shall have potential applications in broad fields.

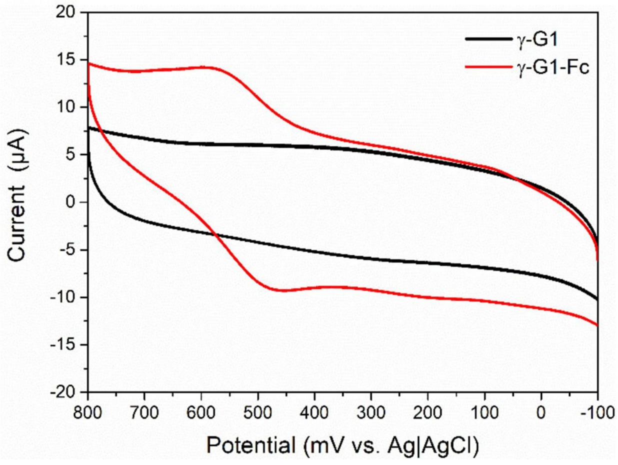

Figure 3. CVs of **γ-G1** and **γ-G1-Fc** in 1.0 M HClO$_4$ at a scan rate of 0.10 V/s.

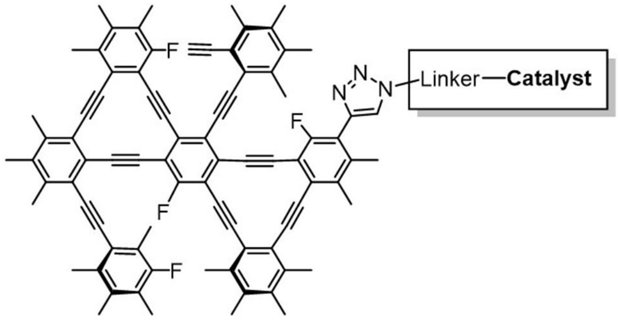

Figure 4. Illustrative structure of **γ-G1** immobilized transition metal catalysts.

Acknowledgements

This work is supported by the National Natural Science Foundation of China (21771098), the State Key Laboratory of Fine Chemicals (KF1802), Shenzhen Clean Energy Research Institute (No. CERI-KY-2019-003) and Shenzhen R&D Fund (KQTD20180411143418361).

Conflict of Interest

The authors declare no conflict of interest.

Keywords: Surface chemistry · Graphyne · Carbon material · Click chemistry · Covalent bond

[1] S. Asmat, A. H. Anwer, Q. Husain, *Int. J. Biol. Macromol.* **2019**, *140*, 484–495.
[2] Z. Cao, S. B. Zacate, X. Sun, J. Liu, E. M. Hale, W. P. Carson, S. B. Tyndall, J. Xu, X. Liu, X. Liu, C. Song, J. H. Luo, M. J. Cheng, X. Wen, W. Liu, *Angew. Chem. Int. Ed.* **2018**, *57*, 12675–12679.
[3] J. Ji, L.-M. Shi, F. Wu, Z.-F. Xin, A.-Q. Jia, Q.-F. Zhang, *J. Coord. Chem.* **2020**, *73*, 1314–1324.
[4] B. Reuillard, K. H. Ly, T. E. Rosser, M. F. Kuehnel, I. Zebger, E. Reisner, *J. Am. Chem. Soc.* **2017**, *139*, 14425–14435.
[5] J. Willkomm, E. Bertin, M. Atwa, J.-B. Lin, V. Birss, W. E. Piers, *ACS Appl. Mater. Interfaces* **2019**, *2*, 4, 2414–2418.
[6] D. H. Nam, P. De Luna, A. Rosas-Hernandez, A. Thevenon, F. Li, T. Agapie, J. C. Peters, O. Shekhah, M. Eddaoudi, E. H. Sargent, *Nat. Mater.* **2020**, *19*, 266–276.
[7] N. Corbin, J. Zeng, K. Williams, K. Manthiram, *Nano Res.* **2019**, *12*, 2093–2125.
[8] X. Cui, W. Li, P. Ryabchuk, K. Junge, M. Beller, *Nature Catal.* **2018**, *1*, 385–397.
[9] K. Tshenkeng, P. Mashazi, *Electrochim. Acta* **2020**, *360*, 137015.
[10] S. Wu, S. Fan, S. Tan, J. Wang, C.-P. Li, *RSC Adv.* **2018**, *8*, 775–784.
[11] F. Duan, M. Hu, C. Guo, Y. Song, M. Wang, L. He, Z. Zhang, R. Pettinari, L. Zhou, *Chem. Eng. J.* **2020**, *398*, 125452.
[12] S. T. Moerz, P. Huber, *Langmuir* **2014**, *30*, 2729–2737.
[13] V. Gascon, I. Diaz, C. Marquez-Alvarez, R. M. Blanco, *Molecules* **2014**, *19*, 7057–7071.
[14] M. Hartmann, X. Kostrov, *Chem. Soc. Rev.* **2013**, *42*, 6277–6289.
[15] E. A. Mohamed, Z. N. Zahran, Y. Tsubonouchi, K. Saito, T. Yui, M. Yagi, *ACS Appl. Mater. Interfaces* **2020**, *3*, 4114–4120.
[16] S. Nisha, A. Senthil Kumar, *ACS Omega* **2020**, *5*, 11817–11828.
[17] X. Zhang, Z. Wu, X. Zhang, L. Li, Y. Li, H. Xu, X. Li, X. Yu, Z. Zhang, Y. Liang, H. Wang, *Nat. Commun.* **2017**, *8*, 14675.
[18] A. F. da Silva, G. S. de Pádua, D. T. de Araújo, C. A. Vieira, E. H. de Faria, *J. Solid State Chem.* **2020**, *287*, 121332.
[19] Z. Li, J. F. R. Van Guyse, V. R. de la Rosa, H. Van Gorp, P. Walke, M. C. Rodríguez González, H. Uji-i, R. Hoogenboom, S. De Feyter, S. F. L. Mertens, *Adv. Funct. Mater.* **2019**, *29*, 1901488.
[20] Z. Liu, H. Zhou, Z. Huang, W. Wang, F. Zeng, Y. Kuang, *J. Mater. Chem. A* **2013**, 1.
[21] L. Tong, M. Gothelid, L. Sun, *Chem. Commun.* **2012**, *48*, 10025–10027.
[22] R. H. Baughman, H. Eckhardt, M. Kertesz, *J. Chem. Phys.* **1987**, *87*, 6687–6699.
[23] Y. Xue, Y. Li, J. Zhang, Z. Liu, Y. Zhao, *Sci. China Chem.* **2018**, *61*, 765–786.
[24] Y. Li, L. Xu, H. Liu, Y. Li, *Chem. Soc. Rev.* **2014**, *43*, 2572–2586.
[25] J. He, N. Wang, Z. Cui, H. Du, L. Fu, C. Huang, Z. Yang, X. Shen, Y. Yi, Z. Tu, Y. Li, *Nat. Commun.* **2017**, *8*, 1172.
[26] X. Shen, Z. Yang, K. Wang, N. Wang, J. He, H. Du, C. Huang, *ChemElectroChem* **2018**, *5*, 1435–1443.
[27] J. He, K. Bao, W. Cui, J. Yu, C. Huang, X. Shen, Z. Cui, N. Wang, *Chem. Eur. J.* **2018** *24*, 1187–1192.
[28] Z. Zuo, H. Shang, Y. Chen, J. Li, H. Liu, Y. Li, Y. Li, *Chem. Commun.* **2017**, *53*, 8074–8077.
[29] L. Hui, Y. Xue, H. Yu, Y. Liu, Y. Fang, C. Xing, B. Huang, Y. Li, *J. Am. Chem. Soc.* **2019**, 141, 10677–10683.
[30] J. Gao, J. He, N. Wang, X. Li, Z. Yang, K. Wang, Y. Chen, Y. Zhang, C. Huang, *Chem. Eng. J.* **2019**, 373, 660–667.
[31] X. Wang, Z. Yang, W. Si, X. Shen, X. Li, R. Li, Q. Lv, N. Wang, C. Huang, *Carbon* **2019**, *147*, 9–18.
[32] Q. Li, Y. Li, Y. Chen, L. Wu, C. Yang, X. Cui, *Carbon* **2018**, *136*, 248–254.
[33] L. Zhao, P. Sang, S. Guo, X. Liu, J. Li, H. Zhu, W. Guo, *Appl. Surf. Sci.* **2017**, *405*, 455–464.
[34] C. Xie, N. Wang, X. Li, G. Xu, C. Huang, *Chem. Eur. J.* **2020**, *26*, 569–583.
[35] Q. Li, C. Yang, L. Wu, H. Wang, X. Cui, *J. Mater. Chem. A* **2019**, *7*, 5981–5990.
[36] A. Ajaz, A. Z. Bradley, R. C. Burrell, W. H. H. Li, K. J. Daoust, L. B. Bovee, K. J. DiRico, R. P. Johnson, *J. Org. Chem.* **2011**, *76*, 9320–9328.
[37] M. Breugst, H.-U. Reissig, *Angew. Chem. Int. Ed.* **2020**, *59*, 12293–12307.
[38] T. Dutta, K. B. Woody, M. D. Watson, *J. of the Am. Chem. Soc.* **2008**, *130*, 452–453.
[39] W. Ding, M. Sun, Z. Zhang, X. Lin, B. Gao, *Ultrason. Sonochem.* **2020**, *61*, 104850.
[40] J. Zhou, X. Gao, R. Liu, Z. Xie, J. Yang, S. Zhang, G. Zhang, H. Liu, Y. Li, J. Zhang, Z. Liu, *J. Am. Chem. Soc.* **2015**, *137*, 7596–7599.
[41] R. Liu, X. Gao, J. Zhou, H. Xu, Z. Li, S. Zhang, Z. Xie, J. Zhang, Z. Liu, *Adv. Mater.* **2017**, *29*, 1604665.
[42] T. Yamashita, P. Hayes, *Appl. Surf. Sci.* **2008**, 254, 2441–2449.
[43] R. Zanoni, A. Aurora, F. Cattaruzza, C. Coluzza, E. A. Dalchiele, F. Decker, G. Di Santo, A. Flamini, L. Funari, A. G. Marrani, *Mater. Sci. Eng. C* **2006**, *26*, 840–845.
[44] J. P. Collman, N. K. Devaraj, T. P. A. Eberspacher, C. E. D. Chidsey, *Langmuir* **2006**, *22*, 2457–2464.
[45] S. Ciampi, P. K. Eggers, G. Le Saux, M. James, J. B. Harper, J. J. Gooding, *Langmuir* **2009**, *25*, 2530–2539.
[46] R. C. Gray, D. M. Hercules, *Inorg. Chem.* **1977**, *16*, 1426–1427.

Manuscript received: February 5, 2021
Revised manuscript received: March 11, 2021
Accepted manuscript online: March 17, 2021
Version of record online: March 22, 2021